

Electrochemical Determination of Chloramphenicol based on ZnO-NPs/SWCNTS Composite modified glassy carbon electrode

Wei Wang^{1,*}, De Sun²

¹ Department of Pharmaceutical Engineering, College of Humanities & Information Changchun University of Technology, Changchun, Jilin 130122, China

² Department of Chemical Engineering, Changchun University of Technology, Changchun, Jilin 130012, China

*E-mail: wangweiccutchi@163.com

Received: 14 September 2020 / Accepted: 26 November 2020 / Published: 31 December 2020

This paper was focused on studying the electrochemical properties of Zinc Oxide nanoparticles (ZnO NPs)/SWCNTs/glassy carbon electrode (GCE) to determine chloramphenicol (CAP) through voltammetric techniques. ZnO NPs/SWCNTs composite was synthesized using sol-gel technique for modification of GCE surface. The morphology and structure of ZnO NPs/SWCNTs was studied by FESEM and XRD analyses. The results indicated that the ZnO NPs were successfully synthesized in wurtzite hexagonal structure on SWCNTs structure. Electrochemical results revealed that ZnO NPs/SWCNTs/GCE possess high stability, selectivity and repeatability response for determination of CAP. The wide linear range, high sensitivity and low detection limit for CAP detection were 10 μ M-140 μ M, 1.65931 μ A/ μ M and 0.03 μ M, respectively. Determination of CAP by ZnO NPs/SWCNTs/GCE sensor in eye drops showed that it can be a suitable choice for practical detection of CAP in real samples.

Keywords: Chloramphenicol; ZnO NPs/SWCNTs composite; Electrochemical sensor; Voltammetric techniques

1. INTRODUCTION

Today, the pharmaceutical industry is one of the most important bases of health and medical services. Huge market of this industry leads to huge investments on research and drug analysis which contribute to study of quality control, safety, performance, stability, toxicology, and side effects of drugs. Therefore, prior to drug development, drug analysis is essential for diagnosis the pharmaceutical formulation and isolation of the active constituent, purification, and standardization of drugs. Many of researches are focused on identification and development of analytical techniques to

obtain the low cost, simple, sensitive, valid and rapid determination methods of trace pharmaceutical elements in blood, food and water. High performance liquid chromatography, gas chromatography, UV/Vis spectrophotometry, NMR spectroscopy, fluorescence, capillary electrophoresis and electrochemical methods are widely used for determination of qualitative and quantitative of pharmaceutical compounds [1, 2]. However, these methods need preliminary preparation of samples, expensive extraction and derivatization processes which make these costly complicated and time-consuming analysis [3, 4]. In the last decades, electrochemical methods have been considered as interesting convenient analysis because of low cost, simplicity, sensitivity and accuracy to determine the organic and inorganic compounds in pharmaceuticals and chemical compositions [5-7].

Chloramphenicol (CAP, {2,2-dichloro-N-[2-hydroxy-1-(hydroxymethyl)-2-(4-nitrophenyl) ethyl] acetamide}; $C_{11}H_{12}Cl_2N_2O_5$) is widely used as antibiotic inhibiting the activity such as Gram-negative, Gram-positive, spirochetes, rickettsiae bacteria and wide broad-spectrum bacteria in food-producing animals. Moreover, this antibiotic is also used in eye drops and eye ointments to treat conjunctivitis. Therefore, these compounds can be released through the human and veterinary medicinal and hospital research wastes. Low cost of CAP makes it a very applicable antibiotic in developing countries. As a consequence, it is observed that toxicity and side effects of CAP causes cancer, leukemia, aplastic anemia, bone marrow suppression, gray baby syndrome, hypersensitivity reactions and neurotoxic reactions which lead to limitation of CAP application in medical science [8]. Therefore, improvement and determination techniques of CAP concentration in pharmaceutical, milk and meat is required.

Many electrochemical studies were performed based on various materials, such as graphene [9], carbon nanotube [10], metallic nanoparticles [11] and nanowires [12, 13], dendrimer [14], composites [15], metal-organic framework [16], and surfactants [17] to development the analytical performance of CAP sensors. However, application of Au nanoparticles decorated graphene oxide [18], CNTs/Cu nanoparticle composite [19] for modification of the CAP sensors showed improvement in sensing properties, no research has been done on this process the analytical performance of ZnO NPs/SWCNTs/ GCE as CAP electrochemical sensor. Therefore, the ZnO NPs/SWCNTs/ GCE sensor was fabricated and applied for the determination of CAP through cycle voltammetry (CV) and differential pulse voltammetry (DPV) techniques.

2. MATERIALS AND METHODS

First step of fabrication of the modified electrode was carboxylation of the single-wall carbon nanotubes (SWCNTs). Therefore, 500 mg of purified SWCNTs (> 90%, Carbon Solutions, Inc., USA) were dispersed in 100 ml of mixture of 3:1 (v/v) H_2SO_4 (96%) and HNO_3 (65%) solution, and ultrasonicated at 20 kHz for 60 minutes at room temperature. The dispersed SWCNTs were filtered with PTFE disk filter (1 μm , polytetrafluoroethylene membrane disc, Pall Corporation, USA) under vacuum. The filtered SWCNTs were washed several times with deionized water. Then, 10 mg of carboxylated SWCNTs were dispersed in 10 ml of N, N-dimethylformamide (DMF, 99.8%, Sigma-Aldrich, USA).

GCE was polished with alumina slurry (1 μm , Electron Microscopy Sciences, USA) on a polishing cloth pad for 20 minutes and washed ultrasonically with deionized water. For further cleaning the GCE surface, the polished electrode was placed in an electrochemical cell which contained 0.1 M H_2SO_4 and applied potential range of -1.5 to 1.5 V vs Ag/AgCl electrode at 100 mV s^{-1} for 5 minutes. Then, GCE was immersed in the prepared suspension of carboxylated SWCNTs for 10 minutes, and then was dried under an infrared lamp (Nanchang Light Technology Exploitation Co. Ltd., China) for 10 minutes.

In order to synthesize the ZnO NPs/SWCNTs composite [20], 1 M hydroxide gel was prepared by hydrolyzing zinc nitrate hexahydrate (99.999%, Sigma-Aldrich, USA). The prepared gel was ultrasonicated for 4 minutes and then 3 ml of formic acid was added to the gel as mineralizer. The SWCNTs/GCE was immersed in the prepared gel for 20 minutes, and then was dried under $200 \text{ }^\circ\text{C}$ in a hot air oven for 24 hours. Finally, after cooling the modified ZnO NPs/SWCNTs/GCE, it was stored in a refrigerator at $6 \text{ }^\circ\text{C}$ for further electrochemical studies.

In order to prepare the real sample, the eye drops (0.5 % CAP, IMRES, Netherlands) were purchased from a local drug store. A 300 μl of eye drops solution was mixed in 10 ml volumetric flask and diluted to a 10 ml with 0.1 M PBS pH 7. A 250 μl of prepared solution was transferred to 10 ml volumetric flask.

The morphology of ZnO NPs/SWCNTs composite was studied through field emission scanning electron microscopy (FE-SEM, JSM 700F, JEOL, Tokyo, Japan). X-ray diffractometer (XRD) operating at 30 mA/ 40 kV with Cu-K α radiation ($\lambda = 0.154051 \text{ nm}$) was applied for crystallinity characterization of ZnO NPs/SWCNTs composite. Electrochemical studies were performed in the electrochemical cell which containing three-electrodes: Ag/AgCl/(sat KCl) as reference electrode, a Pt wire as the counter electrode and (ZnO NPs/SWCNTs/GCE as the working electrode. CV and DPV studies were carried out in potentiostat (PGSTAT128N, MetrohmAutolab B.V., Utrecht, The Netherlands). The electrolyte of electrochemical cell was 0.1 M phosphate buffer solution (PBS) which prepared of H_3PO_4 ($\geq 85\%$, Liuzhou Xianmi Trade Co., Ltd., China) and NaH_2PO_4 ($>99\%$, Sigma-Aldrich, USA). The pH 7 of PBS was adjusted with HCl and NaOH solutions.

3. RESULTS AND DISCUSSION

Figure 1a displays the FESEM image of the synthesized ZnO NPs/SWCNTs composite. As observed, SWCNTs act as substrates for growth ZnO nanoparticles. FESEM image of SWCNTs is shown in Figure 1b. The tubular structure of the CNTs is observed which possess an average length and diameter of 10 μm and 80 nm, respectively. Therefore, high aspect ratio and high porosity of prepared nanostructures can promote the catalytic properties of ZnO/SWCNTs composite.

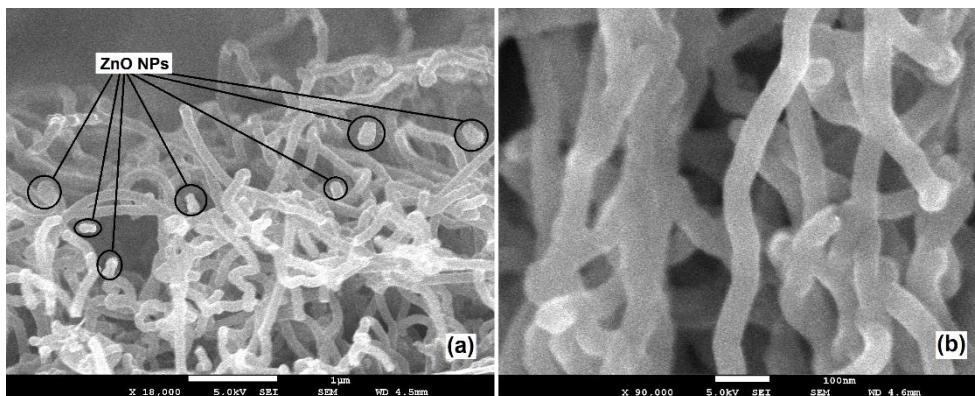


Figure 1. FESEM images of synthesized (a) ZnO/SWCNTs composite and (b) SWCNTs.

The structure of the ZnO NPs, SWCNTs and ZnO NPs/SWCNTs was characterized by XRD analysis. XRD spectrum of ZnO nanostructures in Figure 2 displays diffraction peaks at $2\theta = 31.79^\circ$, 34.48° , 36.28° , 47.68° , 56.67° , 63.02° , 68.11° , and 68.97° which corresponding to the (100), (002), (101), (102), (110), (103), (112), and (201) planes (JCPDS No. 36-1451), respectively[21]. All of these diffraction peaks indicate the highly crystalline of ZnO NPs in wurtzite structure [22]. XRD spectrum of SWCNTs displays peaks at $2\theta = 12.05^\circ$, 25.68° , and 42.97° , which are related to the lattice planes (001), (002), and (100) of graphitic carbon (JCPDS No.41-1487), respectively [23, 24]. The XRD spectrum of the ZnO NPs/SWCNTs exhibits all of ZnO wurtzite structure planes and carbon peaks at $2\theta = 12.79^\circ$ and 24.05° .

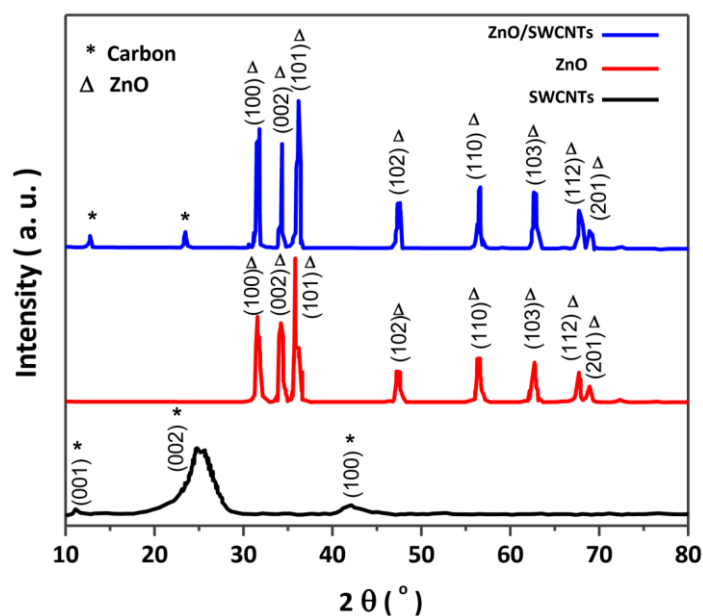


Figure 2. XRD spectrum of ZnO NPs, SWCNTs and ZnO/SWCNTs.

In order to study the electrochemical properties of modified and unmodified electrodes, the CV technique was employed in 0.1 M PBS pH 7.0 at a scan rate of 20 mV s^{-1} in the potential range of -1 to 1.0 V. Figure 3 displayed the electrochemical response of GCE, SWCNTs/GCE and ZnO

NPs/SWCNTs/GCE in absent and present of CAP. As observed, there are no redox peaks for all electrodes in the absence of CAP. After injection of $1\mu\text{M}$ CAP solution in 0.1 M PBS, the CV response of GCE and SWCNTs/GCE show single anodic peak in -0.3 V (Figure 3a-b).

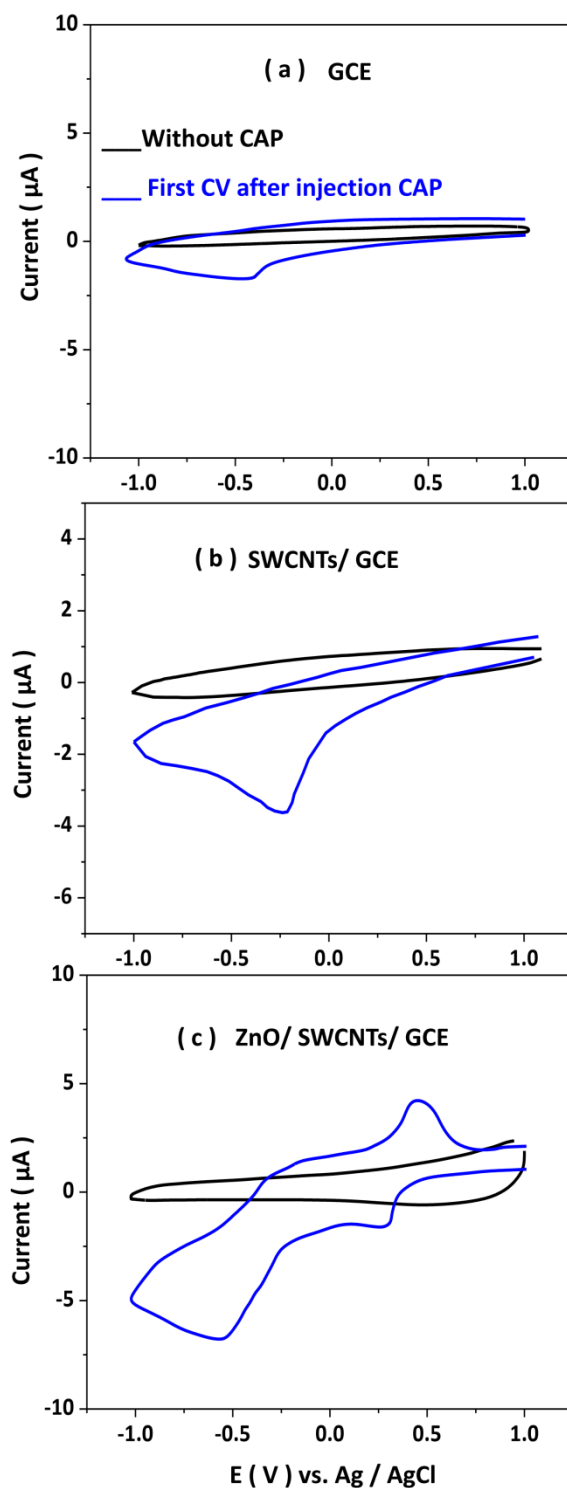


Figure 3. Recorded CVs of (a) bare GCE, (b) SWCNTs/GCE and (c) ZnO NPs/SWCNTs/GCE, respectively, in 0.1 M PBS pH 7.0 at a scan rate of 20 mV s^{-1} in absent and present of $1\text{ }\mu\text{M}$ CAP solution.

As seen, the recorded CV of ZnO NPs/SWCNTs/GCE shows highest current in well-defined single anodic and two cathodic peaks at 0.43 V, 0.27 V and -0.5 V, respectively (Figure 3c). There is the highest cathodic peak at -0.5 V because of four electrons and four proton transfer in direct reduction of the nitro group of CAP to phenyl-hydroxylamine group [25].

Moreover, the single anodic peak at 0.43 V and the lowest cathodic peak at 0.27 V are observed due to the oxidation of hydroxylamine to the nitroso derivative and the reduction of the nitroso derivative to hydroxylamine under two electron and two proton transfer mechanism, respectively [26, 27] (Figure 4).

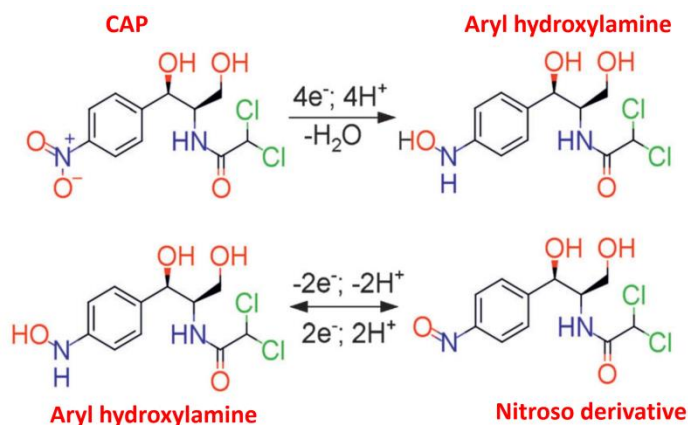


Figure 4. Electrochemical Mechanism of CAP [28]

Therefore, the electrochemical behavior of CAP is dependent on its nitro-aromatic compounds, the number of nitro groups and their position on rings [28-30]. Moreover, it can be seen that GCE and SWCNTs/GCE showed very low peak current and only a cathodic peak at -0.3 V, which indicates the poor electrocatalytic activity of both electrodes to determine CAP. Whereas, ZnO NPs/SWCNTs/GCE is displayed with three peaks and the highest currents of these electrochemical mechanisms because of the synergistic effect of conductive ZnO NPs and SWCNTs and their catalytic roles as mediators in electron transfer of solution onto a GCE surface [31]. In addition, the nanotube structure leads to the creation of a high specific surface area and more active sites on the electrode surface [20]. It is considerable that the cathodic peak current at -0.5 V shows a higher current than other peaks, which indicates a more tendency of the electrocatalytic process to reduce the nitro group and form a hydroxylamine group [28].

Further study was performed to determine the stability of electrode response to the addition of CAP through CV technique. The successive CV response of electrodes in 0.1 M PBS pH 7.0 at a scan rate of 20 mV s^{-1} were recorded. Figure 5 shows the first and 100th recorded CV responses after the addition of $1 \mu\text{M}$ of CAP solution.

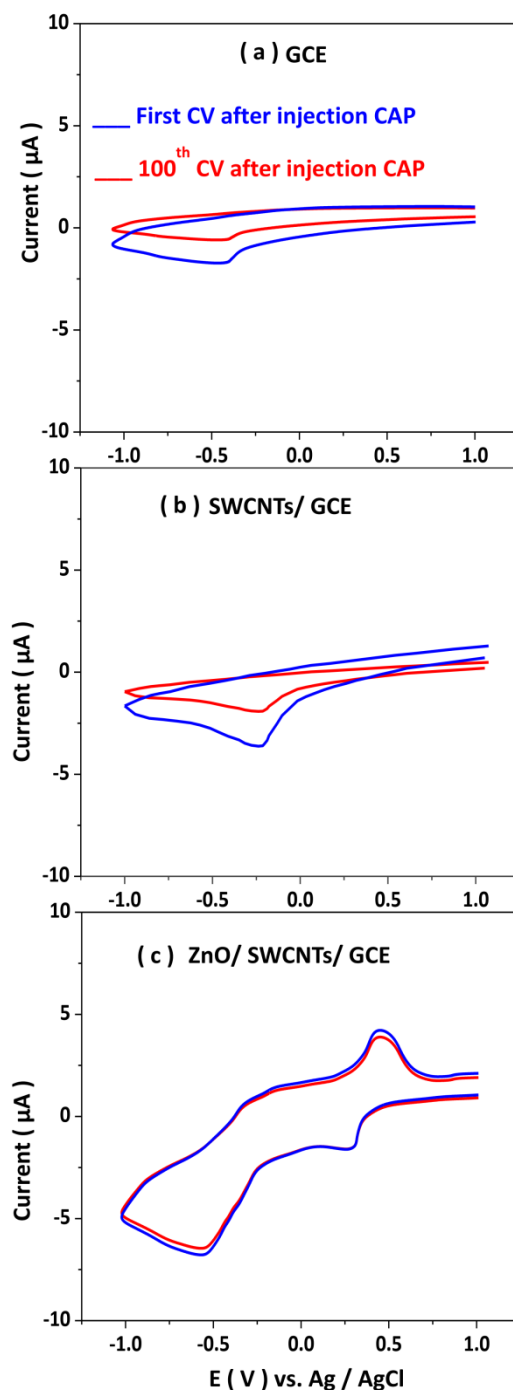


Figure 5. The first and 100th recorded CVs of (a) bare GCE, (b) SWCNTs/GCE and (c) ZnO NPs/SWCNTs/GCE, respectively, in 0.1 M PBS pH 7.0 at a scan rate of 20 mV s⁻¹ in presence of 1 µM CAP solution.

As shown, the decreasing of CAP reduction current after 100 successive CVs at -0.3 V for GCE, SWCNTs/GCE and at -0.5 V for ZnO NPs/SWCNTs/GCE are 67%, 50%, and 6%, respectively. Thus, ZnO NPs/SWCNTs/GCE shows high electrocatalytic current and more stability to determination of CAP. Therefore, this electrode was employed for following electrochemical study as a favorable CAP sensor.

The DPV technique was applied to determine the linear range, detection limit, sensitivity, and selectivity of ZnO NPs/SWCNTs/GCE as CAP sensor. Figure 6a shows the recorded DPV responses of ZnO NPs/SWCNTs/GCE with successive additions of 1 μM CAP solutions in 0.1 M PBS pH 7.0 at a scan rate of 10 mV s^{-1} . The recorded DPVs show an obvious cathodic peak at -0.5 V which is evidence of the electrochemical activity of CAP in solution. Figure 6b displays the calibration plot as an electrocatalytic response to concentration effect of CAP. The detection limit and sensitivity for low concentration of CAP are evaluated 0.03 μM , 0.9876 $\mu\text{A}/\mu\text{M}$, respectively. For determining the linear range of the sensor, this analysis was repeated for additions of 10 μM CAP solutions in electrochemical cells. Therefore, the clearly linear relationship from 10 μM to 140 μM ($R^2 = 0.99807$) is observed in Figure 6c. Moreover, the sensitivity for high concentration of CAP is determined to be 1.65931 $\mu\text{A}/\mu\text{M}$.

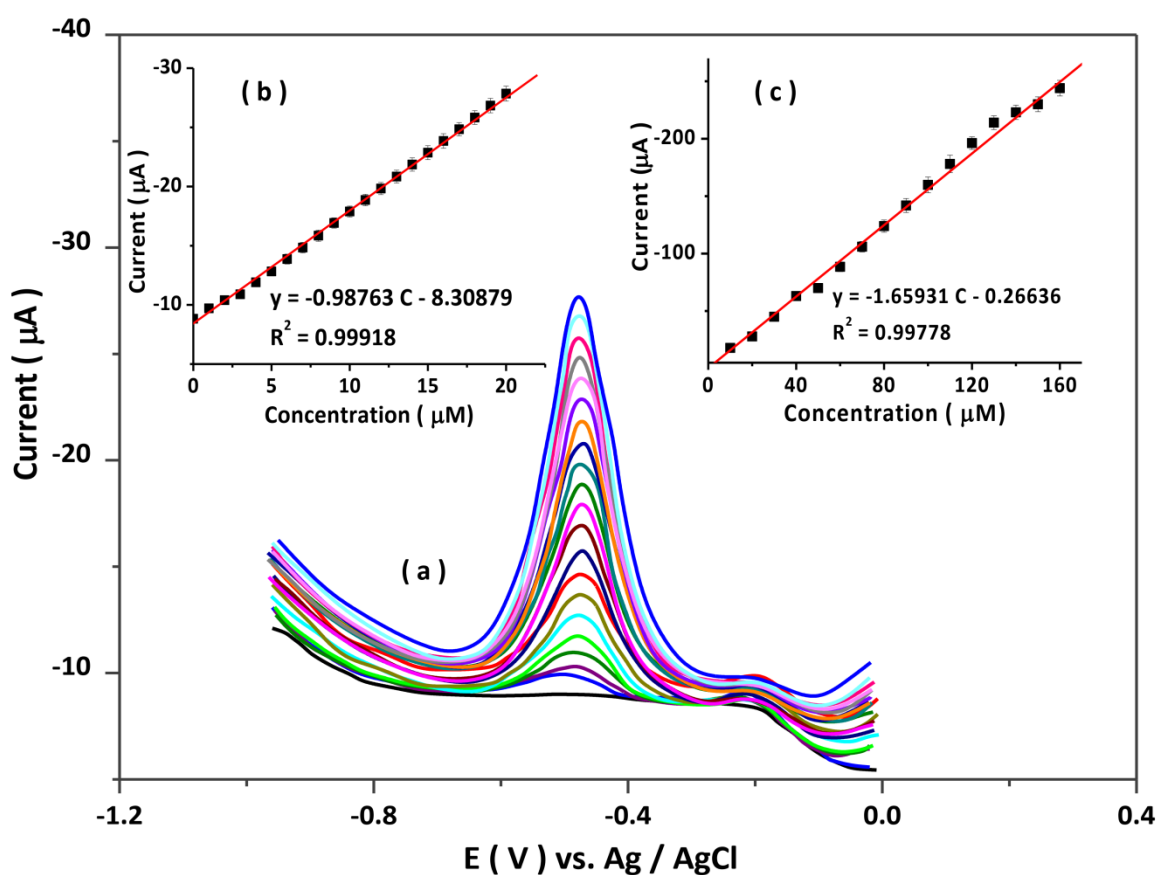


Figure 6. (a) The recorded DPV response of ZnO NPs/SWCNTs/GCE in 0.1 M PBS pH 7.0 at a scan rate of 20 mV s^{-1} in successive additions of 1 μM CAP solution; (b) and (c) the plots of calibration graphs for successive additions of 1 μM and 10 μM CAP solutions, respectively.

Table 1 shows the comparison of detection limit, sensitivity and linear range values of the ZnO NPs/SWCNTs/GCE with other CAP electrochemical sensors for determination of CAP. Results exhibit that MWCNT– cetyltrimethylammonium bromide/GCE [32] and Ag nanodendrites/ShortMWNTs-COOH/GCE[33] show the wider linear range than the ZnO NPs/SWCNTs/GCE. In addition, comparison of the analytical parameters demonstrates that the prepared

sensor performance is better or comparable than these reported electrochemical sensors. It should be considered that this sensor is very stable, low cost and its constituent materials are very environmentally friendly. The suitable electronic properties of SWCNTs together with the ZnO NPs provides the ability to promote charge transfer reactions[34]. Moreover, combination of ZnO NPs and SWCNT with an excellent conductivity coupled with this effect enhanced the electrochemical activity of the prepared modified electrode for CAP determination[34-36].

Table 1. Comparison performance of ZnO NPs/SWCNTs/GCE with other CAP electrochemical sensors.

Electrodes	Technique	detection limit (μM)	Sensitivity ($\mu\text{A}/\mu\text{M}$)	Linear range (μM)	Ref.
ZnO NPs/SWCNTs/GCE	DPV	0.03	1.65931 0.9876	10-140	This work
graphene oxide/ZnO/GCE	DPV	0.01	0.530	0.2–124	[37]
molecularly imprinted polymer /c-MWCNTs-AuNPs/GCE	DPV	0.074	0.0535	0.3–310	[32]
MWCNT- cetyltrimethylammonium bromide/GCE	DPV	0.002	1.948	0.01 –10	[38]
TiN-reduced graphene oxide	CV	0.02	–	0.05–100	[39]
activated carbon fiber microelectrode	SWV*	0.047	0.269	0.1–10	[40]
MoS ₂ -polyaniline nanocomposite	DPV	0.069	0.7656	0.1–100	[41]
3D reduced graphene oxide	DPV	0.150	0.1054	1–113	[42]
Fe ₃ O ₄ -carboxymethyl cellulose/Au	SWV	0.066	3.6277	2.5–25	[28]
AuNPs/graphene oxide	Amperometry	0.250	3.8100	1.5–2.95	[18]
Ag nanodendrites/ShortMWNTs-COOH/GCE	LSSV**	0.049	0.5893	0.3-229	[33]
N-doped graphene/AuNPs	LSV***	0.059	2.13	2–80	[43]

* Square wave voltammetry**Linear sweep stripping voltammetry

***Linear sweep voltammetry

In order to study the selectivity, reproducibility and repeatability response of ZnO NPs/SWCNTs/GCE as CAP sensor, the DPVs responses of modified electrode were recorded in the presence of Al³⁺, Ba²⁺, Ca²⁺, Cd²⁺, Cl⁻, Co²⁺, Cu²⁺, Fe³⁺, Mg²⁺, Mn²⁺, Na⁺, NO³⁻, Zn²⁺, 4-nitrobenzene (4-NB), 4-nitrophenol (4-NP), 4-aminophenol (4-AP), uric acid (UA), glucose (GLU), hypoxanthine (HX), chlortetracycline (CTC), clindamycin (CM), streptomycin (SM) and tetracycline (TC). Figure 7 displays the variation of electrocatalytic current of ZnO NPs/SWCNTs/GCE in 0.1 M PBS pH 7.0 at a scan rate of 20 mV s⁻¹ in successive additions 1 μM of CAP and 10 μM of other analyte solutions. Figure 7 shows a clear response to all additions of CAP solutions before and after addition of the different analytes which indicate the reproducibility and repeatability response of electrodes for detection of CAP. Moreover, it is not observed any considerable response to addition of the other analytes. Therefore, these analytes do not interfere with the determination of CAP on ZnO NPs/SWCNTs/GCE surfaces.

In order to study the practical feasibility of the CAP sensor, the performance of prepared electrode was evaluated in eye drops as a real sample.

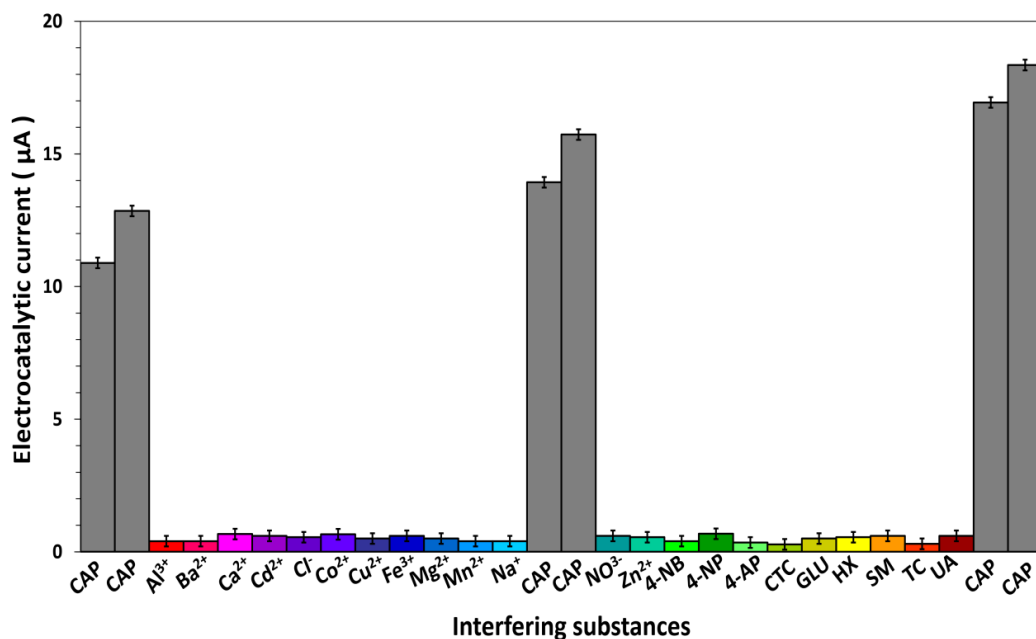


Figure 7. Variation of electrocatalytic current of ZnO NPs/SWCNTs/GCE in 0.1 M PBS pH 7.0 at a scan rate of 20 mV s^{-1} in successive additions $1 \mu\text{M}$ of CAP and $10 \mu\text{M}$ of interfering substance solutions.

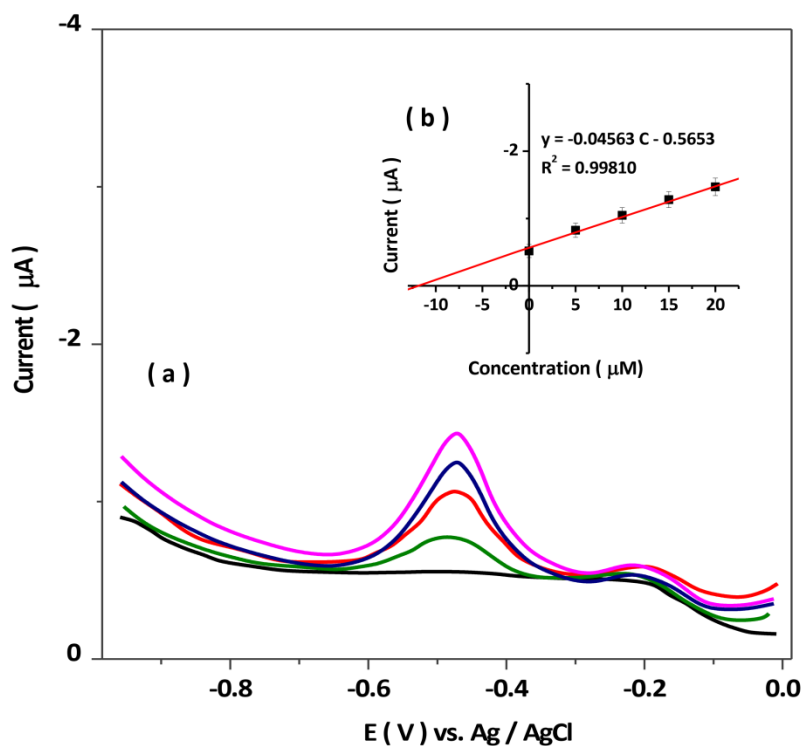


Figure 8. (a) The recorded DPV response of ZnO/SWCNTs/ GCE in 0.1 M PBS pH 7.0 at a scan rate of 20 mV s^{-1} in successive additions of $1 \mu\text{M}$ CAP solution in eye drops; (b) the plots of calibration graphs for determination CAP in eye drops.

The standard addition of the CAP was applied to determine CAP in the real sample through DPV technique (Figure 8a). The calibration plot is presented in Figure 8b. The result shows that the CAP content is obtained 0.4% which is very close to the labeled value (0.5%) with relative standard deviation of 9.2% (n = 4). Therefore, the prepared sensor can be suitable for determination of CAP in real samples.

4. CONCLUSION

In this study electrochemical properties of ZnO NPs/SWCNTs/GCE were investigated for determination of CAP. ZnO NPs/SWCNTs composite was synthesized using sol-gel technique and applied for modification of GCE surface. The FESEM and XRD analyses were applied to study the morphology and structure of ZnO, SWCNTs and ZnO/SWCNTs composite. The voltammetry techniques were used to study the electrochemical properties of ZnO/SWCNTs/ GCE. The FESEM and XRD analyses displayed that high aspect ratio and high porosity ZnO/SWCNTs composite were grown. The electrochemical studies showed that ZnO/SWCNTs/ GCE exhibits high stability, selectivity, and reproducibility and repeatability response to determination of CAP. The wide linear range, high sensitivity and low detection limit were obtained for CAP sensors of 10 to 140 μM , 1.65931 $\mu\text{A}/\mu\text{M}$ and 0.03 μM , respectively. The comparison of the ZnO NPs/SWCNTs/GCE with other CAP electrochemical sensors indicated that the performance of the prepared sensor was comparable or better than the reported electrochemical sensors. The result of study of the prepared sensor to determine the CAP in eye drops as real sample showed the CAP content is obtained 0.4% which is very close to the labeled value (0.5%) with relative standard deviation of 9.2% (n = 4). Therefore, the prepared sensor can be suitable for determination of CAP in real samples.

References

1. A. Kaaviya, *Critical Reviews in Analytical Chemistry*, 48(2018)119.
2. J. Rouhi, S. Mahmud, N. Naderi, C.R. Ooi and M.R. Mahmood, *Nanoscale research letters*, 8(2013)1.
3. M.R. Siddiqui, Z.A. AlOthman and N. Rahman, *Arabian Journal of chemistry*, 10(2017)S1409.
4. R. Dalvand, S. Mahmud and J. Rouhi, *Materials Letters*, 160(2015)444.
5. Z. Savari, S. Soltanian, A. Noorbakhsh, A. Salimi, M. Najafi and P. Servati, *Sensors and Actuators B: Chemical*, 176(2013)335.
6. F. Husairi, J. Rouhi, K. Eswar, C.R. Ooi, M. Rusop and S. Abdullah, *Sensors and Actuators A: Physical*, 236(2015)11.
7. T.A. Ali, G.G. Mohamed, M. Omar and V.N. Abdrabou, *International Journal of Electrochemical Science*, 10(2015)2439.
8. M. Moffa and I. Brook, *Mandell, Douglas, and Bennett's Principles and Practice of Infectious Diseases. 8th ed. Philadelphia: Saunders*, 12(2015)322.
9. R Asadpour, NB Sapari, MH Isa, S Kakooei, *Environmental Science and Pollution Research*, 23(2016)11740.

10. S.A. Zaidi, *International Journal of Electrochemical Science*, 8(2013)9936.
11. J. Rouhi, C.R. Ooi, S. Mahmud and M.R. Mahmood, *Electronic Materials Letters*, 11(2015)957.
12. T. Kokulnathan, T.S.K. Sharma, S.-M. Chen, T.-W. Chen and B. Dinesh, *Journal of the Taiwan Institute of Chemical Engineers*, 89(2018)26.
13. J. Rouhi, S. Kakooei, M. Che Ismail, R. Karimzadeh, M. Rusop Mahmood, *Journal of The Electrochemical Society*, 12(2017)9933.
14. D.-M. Kim, M.A. Rahman, M.H. Do, C. Ban and Y.-B. Shim, *Biosensors and Bioelectronics*, 25(2010)1781.
15. T. Kokulnathan, T.S.K. Sharma, S.-M. Chen and Y. Han-Yu, *Journal of The Electrochemical Society*, 165(2018)B281.
16. L. Xiao, R. Xu, Q. Yuan and F. Wang, *Talanta*, 167(2017)39.
17. W. Zheng, F. Yan and B. Su, *Journal of Electroanalytical Chemistry*, 781(2016)383.
18. R. Karthik, M. Govindasamy, S.-M. Chen, V. Mani, B.-S. Lou, R. Devasenathipathy, Y.-S. Hou and A. Elangovan, *Journal of Colloid and Interface Science*, 475(2016)46.
19. A. Munawar, M.A. Tahir, A. Shaheen, P.A. Lieberzeit, W.S. Khan and S.Z. Bajwa, *Journal of Hazardous Materials*, 342(2018)96.
20. T. Chen and L. Dai, *Materials Today*, 16(2013)272.
21. J. Rouhi, C.R. Ooi, S. Mahmud and M.R. Mahmood, *Materials Letters*, 147(2015)34.
22. H. Savaloni and R. Savari, *Materials Chemistry and Physics*, 214(2018)402.
23. M.M. Reddy, G.R. Reddy, K. Chennakesavulu, E. Sundaravadivel, S. Prasath, A. Rabel and J. Sreeramulu, *Journal of Porous Materials*, 24(2017)149.
24. H. Qin, Y. Huang, S. Liu, Y. Fang, X. Li and S. Kang, *Journal of Nanomaterials*, 2015(2015)1.
25. S. Chuanuwatanakul, O. Chailapakul and S. Motomizu, *Analytical Sciences*, 24(2008)493.
26. M. Feng, D. Long and Y. Fang, *Analytica chimica acta*, 363(1998)67.
27. R. Dalvand, S. Mahmud, J. Rouhi and C.R. Ooi, *Materials Letters*, 146(2015)65.
28. P. Jakubec, V. Urbanová, Z. Medříková and R. Zbořil, *Chemistry—A European Journal*, 22(2016)14279.
29. S. Pilehvar, F. Dardenne, R. Blust and K. De Wael, *International Journal of Electrochemical Science*, 7(2012)5000.
30. J.-C. Chen, J.-L. Shih, C.-H. Liu, M.-Y. Kuo and J.-M. Zen, *Analytical Chemistry*, 78(2006)3752.
31. W. Zhang, T. Yang, D. Huang, K. Jiao and G. Li, *Journal of Membrane Science*, 325(2008)245.
32. H. Zhao, Y. Chen, J. Tian, H. Yu and X. Quan, *Journal of The Electrochemical Society*, 159(2012)J231.
33. P. Zhang, N. Zhang, L. Jing, B. Hu, X. Yang and X. Ma, *International Journal of Electrochemical Science*, 14(2019)9337.
34. T. Madrakian, H. Ghasemi, E. Haghshenas and A. Afkhami, *RSC advances*, 6(2016)33851.
35. P. Li, Y. Liu, J. Liu, Z. Li, G. Wu and M. Wu, *Chemical Engineering Journal*, 271(2015)173.
36. R. Hassanzadeh, A. Siabi-Garjan, H. Savaloni and R. Savari, *Materials Research Express*, 6(2019)106429.
37. N. Sebastian, W.-C. Yu and D. Balram, *Inorganic Chemistry Frontiers*, 6(2019)82.
38. K. Kor and K. Zarei, *Journal of Electroanalytical Chemistry*, 733(2014)39.
39. F.-Y. Kong, T.-T. Chen, J.-Y. Wang, H.-L. Fang, D.-H. Fan and W. Wang, *Sensors and Actuators B: Chemical*, 225(2016)298.
40. L. Agüí, A. Guzmán, P. Yáñez-Sedeño and J.M. Pingarrón, *Analytica Chimica Acta*, 461(2002)65.
41. T. Yang, H. Chen, T. Ge, J. Wang, W. Li and K. Jiao, *Talanta*, 144(2015)1324.
42. X. Zhang, Y.-C. Zhang and J.-W. Zhang, *Talanta*, 161(2016)567.

43. J. Borowiec, R. Wang, L. Zhu and J. Zhang, *Electrochimica Acta*, 99(2013)138.

© 2021 The Authors. Published by ESG (www.electrochemsci.org). This article is an open access article distributed under the terms and conditions of the Creative Commons Attribution license (<http://creativecommons.org/licenses/by/4.0/>).